Journal of Cerebral Blood Flow & Metabolism (2007) 27, 1931–1940

www.jcbfm.com

Soluble epoxide hydrolase: a novel therapeutic target in stroke

Wenri Zhang[1], Ines P Koerner[1], Ruediger Noppens[1], Marjorie Grafe[2], Hsing-Ju Tsai[3], Christophe Morisseau[3], Ayala Luria[3], Bruce D Hammock[3], John R Falck[4] and Nabil J Alkayed[1]

[1]*Department of Anesthesiology & Peri-Operative Medicine, Oregon Health & Science University, Portland, Oregon, USA;* [2]*Department of Pathology, Oregon Health & Science University, Portland, Oregon, USA;* [3]*Department of Entomology and UCD Cancer Center, University of California, Davis, California, USA;* [4]*Department of Biochemistry, UT Southwestern Medical Center, Dallas, Texas, USA*

The P450 eicosanoids epoxyeicosatrienoic acids (EETs) are produced in brain and perform important biological functions, including protection from ischemic injury. The beneficial effect of EETs, however, is limited by their metabolism via soluble epoxide hydrolase (sEH). We tested the hypothesis that sEH inhibition is protective against ischemic brain damage *in vivo* by a mechanism linked to enhanced cerebral blood flow (CBF). We determined expression and distribution of sEH immunoreactivity (IR) in brain, and examined the effect of sEH inhibitor 12-(3-adamantan-1-yl-ureido)-dodecanoic acid butyl ester (AUDA-BE) on CBF and infarct size after experimental stroke in mice. Mice were administered a single intraperitoneal injection of AUDA-BE (10 mg/kg) or vehicle at 30 mins before 2-h middle cerebral artery occlusion (MCAO) or at reperfusion, in the presence and absence of P450 epoxygenase inhibitor *N*-methylsulfonyl-6-(2-propargyloxyphenyl) hexanamide (MS-PPOH). Immunoreactivity for sEH was detected in vascular and non-vascular brain compartments, with predominant expression in neuronal cell bodies and processes. 12-(3-Adamantan-1-yl-ureido)-dodecanoic acid butyl ester was detected in plasma and brain for up to 24 h after intraperitoneal injection, which was associated with inhibition of sEH activity in brain tissue. Finally, AUDA-BE significantly reduced infarct size at 24 h after MCAO, which was prevented by MS-PPOH. However, regional CBF rates measured by iodoantipyrine (IAP) autoradiography at end ischemia revealed no differences between AUDA-BE- and vehicle-treated mice. The findings suggest that sEH inhibition is protective against ischemic injury by non-vascular mechanisms, and that sEH may serve as a therapeutic target in stroke.
Journal of Cerebral Blood Flow & Metabolism (2007) **27,** 1931–1940; doi:10.1038/sj.jcbfm.9600494; published online 18 April 2007

Keywords: cerebral ischemia; CBF; EETs; EPHX2; eicosanoids; neuroprotection; P450 epoxygenase; sEH; stroke

Introduction

We have shown previously that ischemic preconditioning induces the expression of cytochrome P450 epoxygenase in brain, which was associated with a reduction in infarct size after middle cerebral artery occlusion (MCAO) in the rat (Alkayed *et al*, 2002). The P450 epoxygenase metabolizes arachidonic acid into biologically active eicosanoids referred to as epoxyeicosatrienoic acids (EETs). Epoxyeicosatrienoic acids are produced in brain by astrocytes (Alkayed *et al*, 1996*b*) and play an important role in the regulation of cerebral blood flow (CBF) (Alkayed *et al*, 1996*a*) and neurovascular coupling (Alkayed *et al*, 1997). More recently, we showed that EETs reduce cell death induced in astrocytes by oxygen–glucose deprivation (Liu and Alkayed, 2005). The biological activity of EETs is terminated through multiple pathways (Zeldin, 2001), including metabolism by soluble epoxide hydrolase (sEH) into less active vicinal diols referred to as dihydroxyeicosatrienoic acids. However, despite indications for the presence of sEH activity and expression in

Correspondence: Dr NJ Alkayed, Department of Anesthesiology & Peri-Operative Medicine, Oregon Health & Science University, 3181 SW Sam Jackson Park Road, UHS-2, Portland, Oregon 97239-3098, USA.
E-mail: alkayedn@ohsu.edu
This work was supported by NS44313 and NS049210 to NJA. Partial support was provided by GM31278 and the Robert A Welch Foundation to JRF, and ES02710, ES004699 and HL59699-06A1 to BDH.
Received 31 October 2006; revised 8 March 2007; accepted 13 March 2007; published online 18 April 2007

brain (Shin *et al*, 2005), the regional distribution and cellular localization of sEH in brain remain unknown. Furthermore, the precise function of sEH in brain, its role in EETs metabolism, and its contribution to ischemic brain injury have not yet been investigated. In the current study, we characterized for the first time the regional and cellular distribution of sEH immunoreactivity in brain, and tested the hypothesis that sEH inhibition, effectively increasing endogenous brain EETs, is protective against ischemic brain injury *in vivo*. To inhibit sEH, we used 12-(3-adamantan-1-yl-ureido)-dodecanoic acid butyl ester (AUDA-BE), a prototype of newly developed selective inhibitors of sEH (Kim *et al*, 2004; Schmelzer *et al*, 2005). However, it is not clear if these inhibitors cross the blood–brain barrier, and whether they reduce ischemic damage through non-vascular mechanism of action. Therefore, in the current study, we also characterized the pharmacokinetic profile of AUDA-BE and its ability to cross the blood–brain barrier and inhibit sEH enzymatic activity in brain tissue. Finally, we used [^{14}C]iodoantipyrine (IAP) autoradiography to determine if the mechanism of protection by sEH inhibition is linked to increased collateral CBF during vascular occlusion.

Materials and methods

The study was conducted in accordance with the National Institutes of Health guidelines for the care and use of animals in research, and protocols were approved by the Animal Care and Use Committee of Oregon Health and Science University (Portland, OR, USA).

Middle Cerebral Artery Occlusion in Mice

Transient focal cerebral ischemia was induced in adult male C57Bl/6 mice (20 to 26 g, Charles River, Hollister, CA, USA) using the intraluminal MCAO technique, as described previously (Alkayed *et al*, 2001). Briefly, mice were anesthetized with halothane (1.5 to 2% in O_2-enriched air by face mask), and kept warm with water pads. A small laser-Doppler probe was affixed to the skull to monitor cortical perfusion and verify vascular occlusion and reperfusion. A silicone-coated 6-0 nylon monofilament was inserted into the right internal carotid artery via the external carotid artery until laser-Doppler signal dropped to less than 20% of baseline. After securing the filament in place, the surgical site was closed, and the animal was awakened and assessed at 2 h of occlusion for neurological deficit using a simple neurological scoring system as follows: 0 = no deficit, 1 = failure to extend forelimb, 2 = circling, 3 = unilateral weakness, 4 = no spontaneous motor activity. Mice with clear neurological deficit were re-anesthetized, laser-Doppler probe re-positioned over same site on the skull, and the occluding filament was withdrawn to allow for reperfusion. Mice were then allowed to recover and observed for 1 day. Infarct size was measured at 24 h after MCAO in 2-mm thick coronal brain sections (five total) using 2,3,5-triphenyltetrazolium chloride staining and digital image analysis. Sections were incubated in 1.2% 2,3,5-triphenyltetrazolium chloride in saline for 15 mins at 37°C, and then fixed in formalin for 24 h. Slices were photographed, and infarcted (unstained) and uninfarcted (red color) areas were measured with MCID software (InterFocus Imaging Ltd, Linton, UK) and integrated across all five slices. To account for the effect of edema, the infarcted area was estimated indirectly by subtracting the uninfarcted area in the ipsilateral hemisphere from the contralateral hemisphere, and expressing infarct volume as a percentage of contralateral hemisphere. To determine the effect of sEH inhibition on infarct size after MCAO, selective sEH inhibitor AUDA-BE (Schmelzer *et al*, 2005) was administered intraperitoneally 30 mins before MCAO or right after reperfusion (10 mg/kg in 100 μL sesame oil, $n = 5$ per group). To determine if the effect of AUDA-BE is mediated through EETs, AUDA-BE was co-administered with the P450 epoxygenase inhibitor *N*-methylsulfonyl-6-(2-propargyloxyphenyl) hexanamide (MS-PPOH, 0.5 mg/200 μL over 24 h via osmotic minipump, $n = 5$, Brand-Schieber *et al*, 2000). The osmotic pumps (model 2001D; DURECT Corporation, Cupertino, CA, USA) were implanted subcutaneously 24 h before MCAO, and AUDA-BE was administered at the time of reperfusion. They have 8.0 $\pm$ 1.0 μL/h (s.d.) mean pumping rate, which delivers 200 μL mean fill volume over 24-h period. Animals were randomly assigned to treatment groups.

Immunohistochemistry

To localize sEH immunoreactivity in brain, thin coronal sections (6 μm thick) were deparaffinized and heated in 0.5 mmol/L sodium citrate buffer at pH 6.0 in a steamer for 30 mins to intensify staining. Sections were rinsed in Tris-buffered saline (pH 7.6) with 0.1% Triton X-100, and blocked with 3% normal goat serum in phosphate-buffered saline (PBS) with 1% bovine serum albumin and 0.1% Triton for 20 mins at room temperature, followed by an avidin/biotin blocking step. Sections were then incubated with the primary antibody (rabbit anti-sEH, 1:10,000 (Draper and Hammock, 1999) overnight at 4°C. A secondary goat anti-rabbit biotinylated antibody was applied for 30 mins at room temperature, and sections were then incubated with avidin–biotin–peroxidase complex (Vectastain Elite kit, Vector Laboratories, Burlingame, CA, USA) for 30 mins. The color reaction was visualized with diaminobenzidine and sections were lightly counterstained with Mayer's hematoxylin. Sections were dehydrated, overlaid with Permount, then coverslip, and observed with a light microscope. Negative controls were performed by replacing the primary antibody with non-immune rabbit serum and by pre-absorbing the anti-sEH antibody with purified sEH protein.

Isolation of Cerebral Microvessels

To determine the relative distribution of sEH protein in vascular versus non-vascular compartments, cerebral

microvessels were separated from parenchymal brain tissue according to a published protocol (Ospina *et al*, 2002) with slight modifications. Briefly, two mouse brains were pooled, homogenized in ice-cold PBS with a loosely fitting Dounce homogenizer, and centrifuged at 2,000 *g* for 5 mins at 4°C. The supernatant was removed and stored on ice. The pellet was resuspended in PBS and centrifuged at 2,000 *g* for another 5 mins at 4°C. The supernatant was combined with the first supernatant and centrifuged for 10 mins at 3,000 *g* at 4°C. The resulting pellet containing the parenchymal fraction was stored at −80°C. The first pellet was resuspended in PBS, carefully layered over a 15% dextran density gradient (molecular weight 35,000 to 40,000 kDa), and centrifuged in a swinging-bucket rotor for 35 mins at 3,500 *g* at 4°C. The supernatant was discarded, and the pellet was resuspended in PBS, layered over dextran and centrifuged for an additional 35 mins at 3,500 *g*. The resulting pellet was thoroughly washed with ice-cold PBS over a 70 μm nylon mesh and cerebral vessels were collected and stored at −80°C.

Protein Extraction, Sodium Dodecyl Sulfate-Polyacrylamide Gel Electrophoresis, and Western Blot

Brain tissue was homogenized in solution A containing sucrose (250 mmol/L), KCl (60 mmol/L), Tris–HCl (15 mmol/L), NaCl (15 mmol/L), ethylenediamine tetraacetic acid (5 mmol/L), ethylene glycol tetraacetic acid (1 mmol/L), phenylmethanesulfonyl fluoride (0.5 mmol/L), and dithiothreitol (10 mmol/L), then centrifuged at 2,000 *g* for 10 mins at 4°C to isolate cytoplasmic protein. Parenchymal pellets and vessels were processed in a similar manner, except that solution A was supplemented with 0.5% Triton X-100. Protein samples (15 μg) were separated by sodium dodecyl sulfate-polyacrylamide gel electrophoresis and transferred to polyvinylidene difluoride membranes. Blots were then blocked in 5% dry milk and incubated at 4°C overnight with a primary rabbit anti-sEH antibody. Signal was visualized using a biotinylated secondary antibody (Amersham Biosciences, Piscataway, NJ, USA) with an ECL plus (Amersham) chemiluminescence detection kit. Autoradiograms were scanned and band optical densities quantified with QuantityOne® software (BioRad Laboratories, Hercules, CA, USA). Blots were re-probed for the vascular smooth muscle cell marker α-actin (Chemicon International, Inc., Temecula, CA, USA) and for β-actin (Sigma-Aldrich, St Louis, MO, USA) to ensure equal loading.

Soluble Epoxide Hydrolase Activity Assay

To determine if systemically administered AUDA-BE effectively suppresses enzyme activity in brain, sEH activity was determined at 1, 3, 6, and 24 h after drug administration (two animals at each time point, $n = 8$ total per group) using [^{3}H]-*trans*-diphenylpropene oxide (tDPPO) as a substrate (Borhan *et al*, 1995). Rate of hydration of tDPPO is determined by liquid scintillation spectroscopy after differential extraction of the epoxide and diol. Briefly, cytosolic or peroxisomal fractions were incubated at 37°C in 100 nL incubation mixtures containing sodium phosphate buffer (90 mmol/L, pH 7.4) and tDPPO (1 to 50 μmol/L in 1 μL dimethylformamide). Incubations were stopped after 5 mins with the addition of 60 μL methanol and 200 μL isooctane. Zero-time and zero-protein incubations served as blanks. Incubations were vortexed vigorously to extract the substrate into the isooctane (the diol metabolite remains in the aqueous phase). A known aliquot of the aqueous phase was removed and added to 1 mL scintillation cocktail for scintillation counting. Extraction efficiency exceeded 91%.

Regional Cerebral Blood Flow [^{14}C]iodoantipyrine Autoradiography

End-ischemic regional CBF was measured in a non-survival cohort of C57Blk/6 mice using quantitative autoradiography with [^{14}C]IAP, as described previously (Alkayed *et al*, 2001). Two groups of mice (10 mg/kg AUDA-BE given 30 mins before MCAO and vehicle, $n = 5$ per group) were instrumented with femoral artery and jugular vein catheters, and MCA occluded as in the previous cohort. At 2 h of MCA occlusion, 1 μCi of [^{14}C]IAP in 75 μL of saline was infused intravenously for 45 secs. Free-flowing arterial blood was simultaneously sampled at 5-sec intervals for the arterial input function. With the filament in place, mice were decapitated at 45 secs after the start of infusion, and the brain was quickly removed and frozen in 2-methylbutane on dry ice. Brains were sectioned on a cryostat into 20-μm-thick coronal slices, which were thaw-mounted on coverslips and then apposed to film (Kodak, BioMax MR, Eastman Kodak Company, Rochester, NY, USA) with ^{14}C standards for 3 weeks. The concentration of [^{14}C]IAP in blood was determined by liquid scintillation spectroscopy (Beckman 6500) after decolorization with 0.2 mL of tissue solubilizer (Soluene-350, PerkinElmer, Waltham, MA, USA). Autoradiographic images representing five different coronal levels (+2, +1, 0, −1, and −2 mm from Bregma, 3 images each) were digitized, and regional CBF was determined in specific regions with the use of image analysis software (MCID, 7.0). Additionally, areas perfused with specific regional CBF rates were isolated by digital image scanning and summed to construct a histogram distribution of brain tissue over incremental ranges of blood flow rates. Areas were averaged among two images and were integrated across five coronal levels to calculate brain tissue volumes perfused with particular flow rates.

Pharmacokinetic Parameters of Soluble Epoxide Hydrolase Inhibitors

12-(3-Adamantan-1-yl-ureido)-dodecanoic acid butyl ester was dissolved in sesame oil and administered as a single intraperitoneal injection of 10 or 40 mg/kg to C57Bl/6 mice (20 to 26 g). A second set of animals was injected with sesame oil alone (vehicle). Two mice from each treatment were decapitated; blood samples were collected at 1, 3, 6, and 24 h after administration. 12-(3-Adamantan-1-yl-

ureido)-dodecanoic acid butyl ester, its equally active metabolite 12-(3-adamantan-1-yl-ureido)-dodecanoic acid (AUDA) and the inactive metabolite 12-(3-adamantan-1-yl-ureido)-butyl acid (AUBA) were measured in blood samples as described previously (Morisseau *et al*, 2002; Watanabe *et al*, 2006). Briefly, blood samples (10 μL) were collected in 1.5 mL Eppendorf microcentrifuge tubes, weighed, and vortexed with 100 μL of purified water. Samples were spiked with a surrogate compound (1-adamantyl-3-decyl urea, 790, 100 ng/mL) and extracted twice with 500 μL ethyl acetate, dried under nitrogen, and reconstituted in 25 μL of methanol containing 1-cyclohexyl-3-tetradecyl urea (500 ng/ml) as internal standard. Aliquots (10 μL) were analyzed by liquid chromatography coupled mass spectroscopy LC-MS/MS (Watanabe *et al*, 2006; Watanabe and Hammock, 2001).

The concentration of sEH inhibitors were quantified in extracts using HPLC with positive mode electrospray ionization and tandem mass spectrometry. Analytes were quantified on a 5-point curve with internal standard methods. Surrogate recoveries were evaluated by quantification against the internal standard. Surrogate recoveries were 70% for all reported plasma samples, the analysis of reagent blanks, matrix spikes, and analytical replicates were used to document method stability during this study. Molecular ion and transition ion for sEH inhibitors were as follows: AUDA-BE (449.2 > 272.2), AUDA (393.1 > 135), AUBA (281.2 > 104). Transition ions for the surrogate compound 790 was 335.1 > 135 and internal standard 1-cyclohexyl-3-tetradecyl urea was 341.2 > 216.2.

Statistical Analysis

Differences in infarct size, enzyme activity, and blood flow rates were analyzed with a *t*-test for two groups and analysis of variance with *post hoc* Newman–Keuls multiple range test for multiple groups. The pharmacokinetic profile was examined for goodness of fit to a non-compartmental or multicompartmental models. Then pharmacokinetic parameters were obtained by fitting the blood-concentration-time data to a non-compartmental model with the WinNonlin software (Pharsight, Mountain View, CA, USA), as described previously (Watanabe *et al*, 2006). The criterion for statistical significance was set at $P < 0.05$. All values are reported as mean $\pm$ s.e.m.

Results

To determine if sEH is differentially expressed in cerebral blood vessels and brain parenchyma, we fractionated brain tissue into vascular and non-vascular compartments and probed both compartments with anti-sEH antibody. Figure 1 shows that sEH immunoreactivity (62.5 kDa) is found in both compartments. However, in brain, sEH is predominantly localized in the parenchymal fraction, and to a lesser extent in the vascular compartment, as identified by the vascular smooth muscle marker α-actin (40 kDa). We further examined this observation using immunohistochemistry. Figure 2 shows that sEH is abundantly expressed in brain, especially in areas relevant to the stroke model used in the current study, such as the cerebral cortex (A), and striatum (D). Immunoreactivity was predominantly localized in neurons (arrows in C), and it did not co-localize with the astrocyte marker glial fibrillary acidic protein (GFAP, not shown). Within neurons, sEH immunoreactivity was observed in neuronal cell bodies (dotted arrows in C) and dendrites (solid arrows in C). The most striking finding, however, was the localization of sEH immunoreactivity in axons (fine intersecting processes within neuropil in C) and nerve fiber bundles within gray (arrows in B and D) and white matter (upper arrow in D). Notably, in the striatum (D), immunoreactivity was not observed in neuronal cell bodies and was primarily localized in fiber bundles (cross-sections in D). Less consistent immunoreactivity was seen in vascular cells and in cells morphologically consistent with microglia (data not shown). No staining was observed when the primary antibody was removed, and pre-absorbing anti-sEH antibody with purified sEH protein completely eliminated staining.

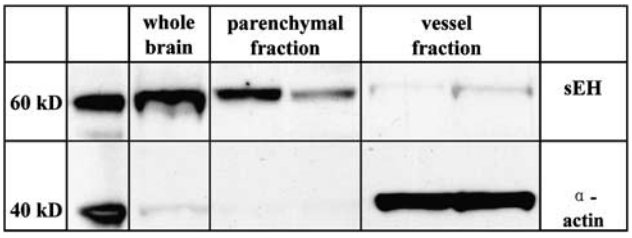

Figure 1 Soluble epoxide hydrolase (sEH) expression in brain. Western blot analysis of brain vascular and non-vascular compartments shows that sEH is predominantly expressed in brain's parenchymal, and to a lesser degree in cerebral vessels. Vascular smooth muscle α-actin is restricted to the vessel fraction, suggesting effective separation of both compartments. Western blot is representative of three blots.

To determine blood concentrations of AUDA-BE and its active metabolite AUDA as well as its inactive indicator metabolite (AUBA) pharmacokinetic studies were performed after a single intraperitoneal injection of 10 and 40 mg/kg AUDA-BE. A time-dependent analysis of plasma sEH inhibitor levels is summarized in Figure 3. 12-(3-Adamantan-1-yl-ureido)-dodecanoic acid butyl ester reached a maximum concentration of 2 μmol/L within the first hour after 40 mg/kg injection (Figure 3A). However, when 10 mg/kg AUDA-BE was injected, only the metabolites AUDA and AUBA were detected (Figure 3B). 12-(3-Adamantan-1-yl-ureido)-dodecanoic acid butyl ester was rapidly hydrolyzed to AUDA and reached maximum concentration of 4 μmol/L within the first hour (Figure 3A). AUDA and AUDA-BE were further degraded to AUBA. 12-(3-Adamantan-1-yl-ureido)-butyl acid (5 μmol/L) was observed in

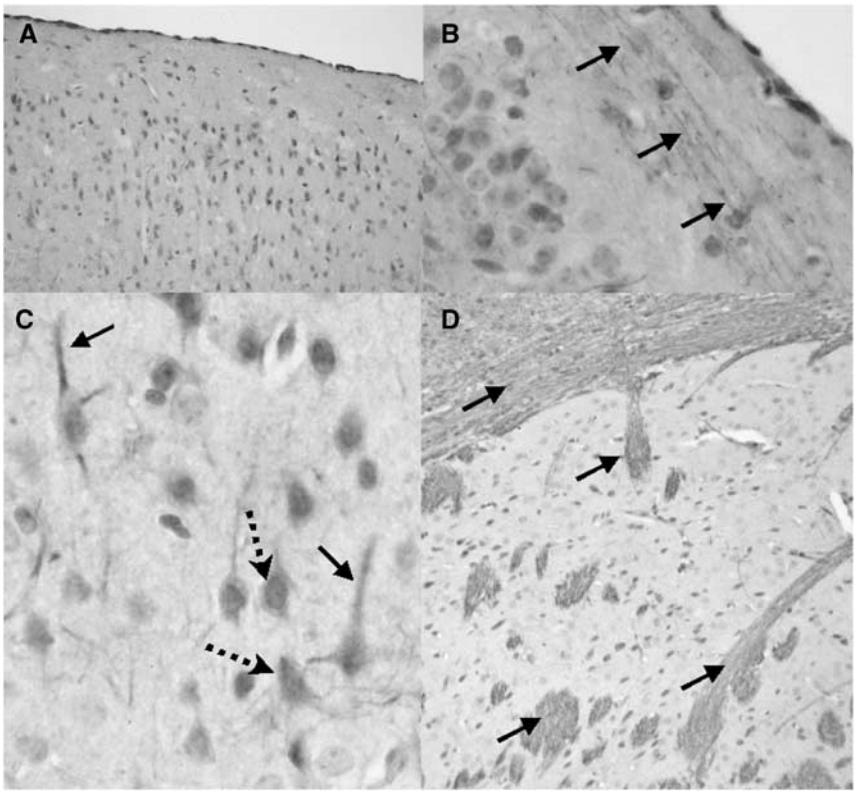

Figure 2 Localization of soluble epoxide hydrolase (sEH) immunoreactivity in mouse brain neuronal cell bodies and processes. Immunoreactivity for sEH in the cerebral cortex (**A** to **C**) and striatum (**D**) is localized to neuronal cell bodies (dotted arrows) and processes (solid arrows). Three immunohistochemistry runs were performed on $n = 3$ mice.

the first hour and the concentration remained relatively stable at 3.5 μmol/L for 24 h after injection (Figure 3A). Figure 3B shows that, when administrated at 10 mg/kg, AUDA-BE is rapidly metabolized, and that its active metabolite AUDA reaches a peak concentration of 52 nmol/L at 1 h, with a slow degradation rate over 24 h, whereas AUBA reaches a higher peak of 113 nmol/L at 3 h, followed by a faster degradation rate over 24 h. No apparent adverse effects were noted for either 10 or 40 mg/kg doses during the 24-h period after drug administration. As the 10-mg/kg dose gives adequate blood levels and clear one-compartment pharmacokinetics, subsequent biological studies were performed with this dose. Pharmacokinetic parameters of AUDA in plasma are summarized in Supplementary Table S1. These data show a maximum concentration of AUDA at 52 nmol/L within 1 h, a half time of elimination of 7 h and a mean residence time of 9 h (Supplementary Table S1).

Previously, we have shown that IC_{50} values of AUDA-BE and AUDA are similar and are in the low nanomolar range (Kim *et al*, 2007; Morisseau *et al*, 2002). This concentration was also biologically effective in lowering blood pressure in hypertensive model (Imig *et al*, 2005). Therefore, in these experiments, the levels of sEH inhibitors in the blood are in the concentration range expected to inhibit the enzyme. To determine if AUDA-BE and its active metabolite cross the blood–brain barrier and reach adequate inhibitory concentrations, we measured AUDA-BE and its metabolites in brain tissue extracted with methanol and chloroform (Folch *et al*, 1951). Although the variability of the inhibitor concentrations was high and the recovery of the compounds was low, significant levels of the active metabolite AUDA, but not the prodrug AUDA-BE or the inactive metabolite AUBA, were detected in homogenates of brain tissue (Supplementary Figure S1). AUDA reached its maximum concentration within 3 h after a single injection of 10 mg/kg AUDA-BE with a mean residence time of 6 h and half-time elimination of 4 h (Supplementary Table S1).

To determine if these concentrations produce adequate inhibition of enzyme activity in brain, sEH hydrolase activity was measured in brain at 1, 3, 6, and 24 h after AUDA-BE administration (10 mg/kg intraperitoneally, $n = 2$ per group at each time point) using sEH-specific substrate [^{3}H]-*trans*-diphenylpropene oxide (tDPPO). Brain sEH activity was significantly inhibited by AUDA-BE, and at least 20% inhibition persisted for up to 24 h (Figure 4). It should be noted that these sEH inhibitors are reversible transition state inhibitors. Thus, the levels of inhibition are certain to be above those

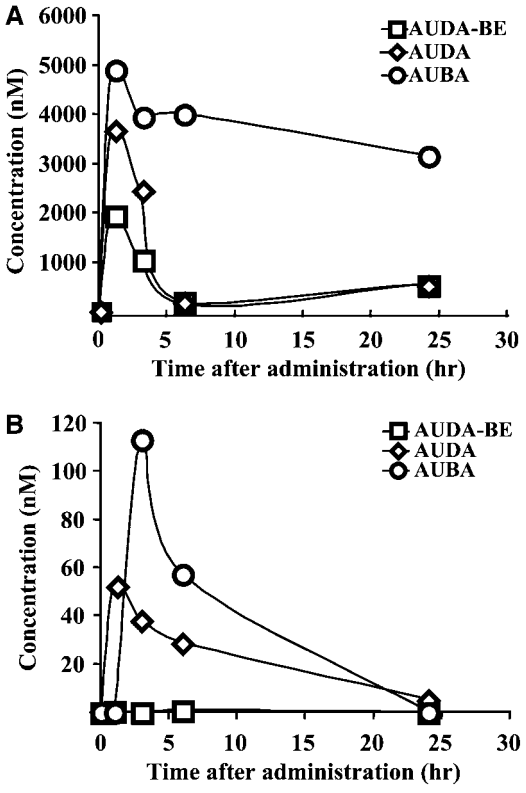

Figure 3 Pharmacokinetic profile of sEH inhibitor AUDA-BE and its metabolites in plasma. AUDA-BE was administered to mice as a single intraperitoneal injection of either 40 mg/kg **(A)** or 10 mg/kg **(B)**. 12-(3-Adamantan-1-yl-ureido)-dodecanoic acid butyl ester and the metabolites AUDA and AUBA were analyzed at 1, 3, 6, and 24 h after injection. Control injections of sesame oil without AUDA-BE led to concentrations of parent drug or metabolites below the detection limits (0.96, 1.10, and 5.78 nmol/L for AUDA, AUDA-BE, and AUBA, respectively). Control values were subtracted from corresponding values at each time point. AUBA is a biologically inactive indicator metabolite. The mean value at each time point represents two animals.

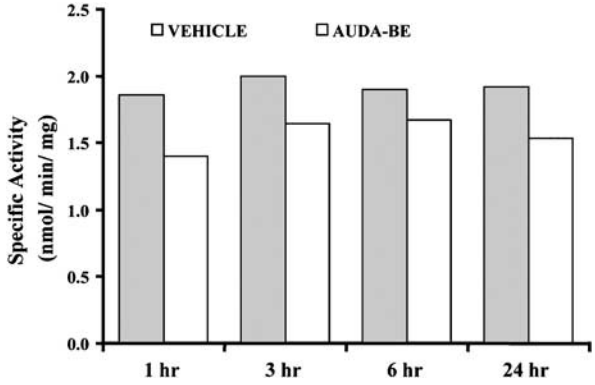

Figure 4 12-(3-Adamantan-1-yl-ureido)-dodecanoic acid butyl ester inhibits soluble epoxide hydrolase enzymatic activity in mouse brain tissue after systemic administration. Activity was measured at 1, 3, 6, and 24 h after single AUDA-BE administration (10 mg/kg intraperitoneally) using sEH-specific surrogate substrate [^{3}H]-*trans*-1,3-diphenylpropene oxide (tDPPO). Average activity over 24 h was reduced from 1.92 $\pm$ 0.06nmol/mg in vehicle-treated mice to 1.56 $\pm$ 0.13 nmol/mg protein in AUDA-BE-treated mice ($n = 2$) at each of four time points: 1, 3, 6, and 24 h after injection, $P < 0.05$.

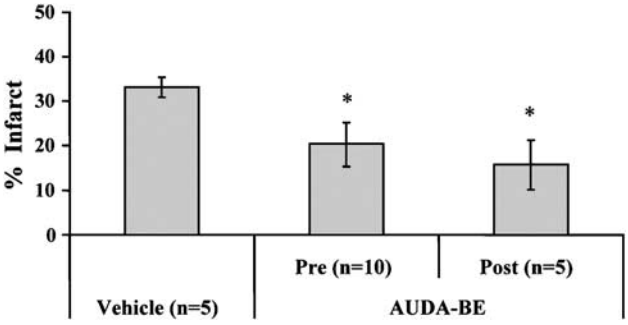

Figure 5 12-(3-Adamantan-1-yl-ureido)-dodecanoic acid butyl ester decreases infarct size after middle cerebral artery occlusion (MCAO) in mice. Infarct size was reduced from 33 $\pm$ 2% ($n = 5$) in vehicle-treated mice to 20 $\pm$ 5% ($n = 10$) and 16 $\pm$ 6% ($n = 5$) when AUDA-BE was administered (10 mg/kg intraperitoneally) 1 h before (pre) or at the time of reperfusion (post) after 2-h MCAO. *Different from vehicle ($P < 0.05$).

detected due to dilution of the sample during work up. Having established the effectiveness and bioavailability of AUDA-BE in brain tissue, we set out to determine its effect on ischemic brain injury. Figure 5 summarizes the effect of AUDA-BE on infarct size after MCAO in mice. Compared with vehicle, AUDA-BE (10 mg/kg) reduced infarct size after 2-h MCAO by 40 and 50% when administered 1 h before (pre, $n = 5$ per group) or at the time of reperfusion (post, $n = 5$ per group), respectively ($P < 0.05$).

To determine if the protection observed by sEH inactivation is linked to EETs, we co-administered AUDA-BE with MS-PPOH, which inhibits EETs biosynthesis via the P450 epoxygenase pathway (Brand-Schieber *et al*, 2000). To ensure adequate inhibition of EETs synthesis and depletion of already formed EETs, MS-PPOH (0.5 mg/200 μL) was administered over 24 h before MCAO. 12-(3-Adamantan-1-yl-ureido)-dodecanoic acid butyl ester was administered as a single intraperitoneal injection (10 mg/kg) at the time of reperfusion. Figure 6 shows that MS-PPOH blocks infarct size reduction by AUDA-BE. When administered alone, AUDA-BE reduces infarct size from 33 $\pm$ 2% to 16 $\pm$ 6% ($n = 5$ per group, $P < 0.05$). However, when combined with MS-PPOH, AUDA-BE loses its protective effect (infarct size 34 $\pm$ 7%, $n = 5$, which is not different from vehicle), which is not attributable to a non-specific effect of MS-PPOH, because MS-PPOH alone (24 $\pm$ 6%, $n = 5$) does not increase infarct size after MCAO.

We then used [^{14}C] IAP autoradiography to determine if AUDA-BE alters CBF during vascular occlusion. Figure 7A is color-coded distribution of CBF in ischemic and contralateral hemispheres, and

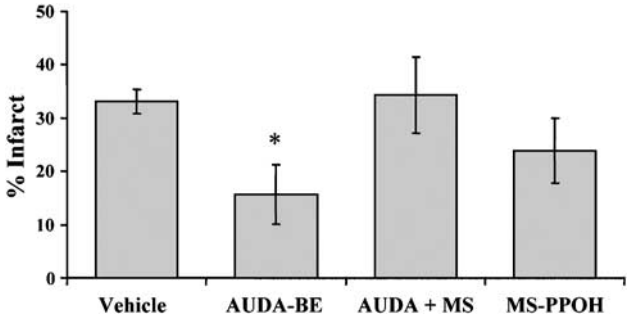

Figure 6 P450 epoxygenase inhibitor *N*-methylsulfonyl-6-(2-propargylloxyphenyl) hexanamide (MS-PPOH) eliminates protection by AUDA-BE. Infract size was reduced by AUDA-BE alone (10 mg/kg, a single intraperitoneal injection at reperfusion) from 33±2% to 16±6% ($n = 5$ per group). However, when combined with MS-PPOH (0.5 mg/200 μL over 24 h before MCAO, via subcutaneously implanted osmotic minipumps), AUDA-BE loses it protective effect (infarct size 34±7%, $n = 5$, not different from vehicle). *Different from vehicle ($P < 0.05$).

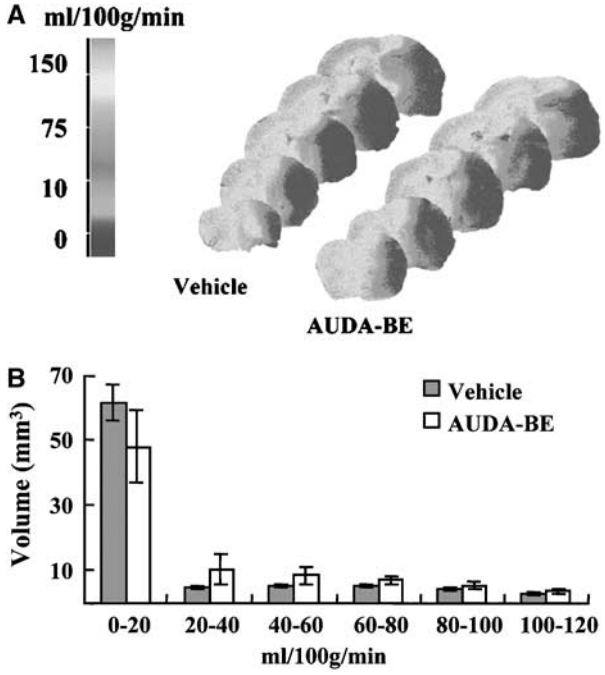

Figure 7 Blood flow rates distribution in mouse brain during MCAO. Flow rates were quantified by [^{14}C]-iodoantipyrine (IAP) autoradiography at the end of 2-h MCAO in mice treated with vehicle (sesame oil, $n = 5$) or AUDA-BE (10 mg/kg intraperitoneally, 30 mins before MCAO, $n = 5$). (**A**) Color-coded distribution of regional CBF rates. (**B**) Blood flow distribution in the ipsilateral hemisphere. No differences were observed in the amount of tissue (mm^3) perfused with any given flow rate (mL/100 g per min) between vehicle- and AUDABE-treated mice ($n = 5$ per group).

Figure 7B is histogram distribution of brain tissue volume over 20 mL/100 g per min increments of CBF rates. Figure 7B shows that regional CBF distribution within the ipsilateral hemisphere at the end of 2-h MCAO was not different between AUDA-BE and vehicle-treated animals ($n = 5$ per group), suggesting that protection by AUDA-BE is not related to altered ischemic severity.

Discussion

We report the following new findings: (1) sEH is expressed at high levels and is highly active in rodent brain, (2) the predominant localization of sEH in brain is in neuronal cell bodies and processes, and to a lesser degree in cerebral blood vessels, (3) inhibition of brain sEH is protective against ischemic brain damage, (4) the mechanism of protection is linked to the P450 epoxygenase, but it is not mediated through increased CBF during vascular oclusion. The findings suggest that sEH is an important player in ischemic brain injury and may serve as a novel therapeutic target in stroke.

Soluble epoxide hydrolase catalyzes the addition of water molecules to epoxides to form corresponding diols (Newman *et al*, 2005). In humans (Enayetallah *et al*, 2004) and rodents (Yu *et al*, 2004; Zheng *et al*, 2001), sEH has been detected in a variety of tissues, including brain (Shin *et al*, 2005). However, the cellular localization of sEH and its distribution in brain regions are unknown. We show here that sEH protein is abundantly expressed in the cerebral cortex and striatum, and that expression is predominantly localized in neuronal cell bodies and processes. Immunoreactivity for sEH did not co-localize with glial fibrillary acidic protein, suggesting that sEH is not expressed in astrocytes. However, in agreement with a vascular localization in kidney (Yu *et al*, 2004), lung (Zheng *et al*, 2001), and other tissues, we also observed sEH immunoreactivity in cerebral blood vessels. It is not clear if vascular versus neuronal sEH plays differential roles in brain function and disease; however, cell-specific localization suggests that sEH may play important roles in regulating neuronal function and CBF.

Soluble epoxide hydrolase is a bifunctional enzyme with hydrolase activity residing in the C-terminus and phosphatase activity in the N-terminus (Newman *et al*, 2003). Most known sEH functions, however, are attributed to its hydrolase activity, especially the hydration of cytochrome P450 eicosanoids referred to as EETs. Epoxyeicosatrienoic acids are produced in brain and astrocytes (Alkayed *et al*, 1996*b*) and exert a variety of physiological functions, including release of hypothalamic hormones (Junier *et al*, 1990), CBF regulation (Alkayed *et al*, 1997), and protection from ischemic cell death (Liu and Alkayed, 2005). Furthermore, we showed previously that ischemic preconditioning, a neuroprotective strategy, induces the expression of EETs-synthesizing enzyme in brain (Alkayed *et al*, 2002) and astrocytes (Liu and Alkayed, 2005), suggesting that EETs may serve as endogenous neuroprotectants against ischemic brain injury. The biological activity of EETs is terminated

via multiple pathways, including hydration into dihydroxyeicosatrienoic acids by sEH (Zeldin, 2001). Therefore, in the current study, we tested the hypothesis that sEH inhibition, effectively increasing endogenous tissue levels of EETs, is protective against ischemic brain injury. To inhibit sEH, we used AUDA-BE, which belongs to a group of newly developed potent, selective, and metabolically stable sEH inhibitors (Kim *et al*, 2004). Similar inhibitors have been used *in vivo* to treat systemic inflammation (Schmelzer *et al*, 2005) and hypertension-related kidney damage (Zhao *et al*, 2004). In the current study, we found that the potent sEH inhibitor AUDA-BE or its active metabolite, AUDA, is capable of crossing blood–brain barrier and effectively suppressing brain sEH enzymatic activity. 12-(3-Adamantan-1-yl-ureido)-dodecanoic acid butyl ester was administered in our study as a single intraperitoneal injection of 10 or 40 mg/kg AUDA-BE, and demonstrated to remain in plasma in its active form as AUDA above the IC_{50} for the rodent enzyme *in vitro* (Kim *et al*, 2007; Morisseau *et al*, 2002). All stroke experiments were performed at a dose of 10 mg/kg parent compound AUDA-BE; the pharmacokinetic profile presented for 40 mg/kg AUDA-BE was presented only to illustrate that the parent compound AUDA-BE can be detected in blood and hydrolyzed into an active inhibitor AUDA. These concentrations of AUDA were shown previously to have biological effects in lowering blood pressure in hypertensive rat models (Imig *et al*, 2005).

Effective enzyme inhibition and bioavailability in brain tissue is further supported by measurements of sEH-specific activity in brain after AUDA-BE or vehicle administration, which show that more than a 20% residual inhibition of sEH activity persisted in brain tissue for up to 24 h. It is important to note that the degree of inhibition *in vivo* is likely to be much higher than 20%. The residual activity reflects remaining inhibition *ex vivo* after tissue homogenization and washout, which dilutes and releases AUDA-BE from sEH, since inhibition is kinetically reversible and AUDA-BE is not covalently bound to sEH. Nevertheless, the data suggest that AUDA-BE enters the brain after systemic administration, inhibits sEH enzyme activity in brain and the inhibition is sustained for 24 h after a single intraperitoneal injection. Possibly, the relatively high levels of AUDA in the brain come from AUDA-BE penetrating into the brain and then being hydrolyzed to AUDA, which does not penetrate cell membranes as readily. More importantly, AUDA-BE significantly reduced infarct size after MCA occlusion in mice, whether it was given before or after MCA occlusion. The efficacy of after ischemic administration of AUDA-BE suggests that the inhibitor acts during reperfusion, and that tissue protection is not a consequence of reduced severity of ischemia. One limitation of our study is that infarct size was measured only at 24 h of reperfusion. Therefore, it is important to determine in future studies if the protective effect of AUDA-BE is long lasting.

Our previous work (Liu and Alkayed, 2005) and a variety of other studies (Liu *et al*, 2004) demonstrating EETs protective effect against ischemic cell death, and the blockade of the effect of AUDA-BE by MS-PPOH support the hypothesis that the mechanism of neuroprotection by AUDA-BE is linked to stabilization of endogenous EETs. It is not clear, however, if sEH inhibitors act exclusively through vascular mechanisms, and whether brain tissue bioavailability is required for ischemic neuroprotection by sEH inhibitors. The observation that MS-PPOH did not alter infarct size after MCAO suggests that EETs synthesis in normal brain is usually low. However, the amount of bioavailable EETs can be augmented by preventing their metabolism through sEH.

Because AUDA-BE is presumed to act through EETs, which are known vasodilators, we further confirmed the lack of effect of AUDA-BE on regional cerebral blood flow during MCA occlusion using [^{14}C]IAP autoradiography. Absolute CBF rates as well as regional blood flow distribution throughout the ischemic hemisphere were similar at end ischemia between AUDA-BE and vehicle-treated mice, suggesting that the mechanism of protection by AUDA-BE is not mediated through vascular mechanisms that alter ischemic severity, although we cannot exclude the possibility that AUDA-BE improved blood flow during the reperfusion period. This is in agreement with our previous study demonstrating that P450 epoxygenase upregulation by ischemic preconditioning is associated with tissue protection from ischemia without increased CBF (Alkayed *et al*, 2002). This conclusion is further supported by the observation that AUDA-BE remained protective against ischemic damage when administered after MCAO.

In addition to their effects on the vasculature, EETs possess other properties that can potentially explain the protective effect of AUDA-BE. For example, EETs have been shown to suppress inflammation (Node *et al*, 1999), hyperthermia (Kozak *et al*, 2000), platelet aggregation (Krotz *et al*, 2004), generation of reactive oxygen species (ROS) (Spiecker and Liao, 2005) and apoptosis (Chen *et al*, 2001), all of which are known to exacerbate ischemic brain injury. Furthermore, EETs have been linked to blood pressure homeostasis and activation of multiple cell survival pathways, including the opening of mitochondrial ATP-dependent potassium channel (mt-K_{ATP}) (Seubert *et al* 2004) and activation of phosphatidylinositol 3-kinase (PI3-K)/AKT (Potente *et al*, 2003) and mitogen-activated protein kinase (MAPK) pathways (Fleming *et al*, 2001). Finally, accumulating evidence suggests that EETs may exert their actions through membrane-associated receptors. Specific high-affinity membrane binding sites for EETs have

been described, although no such receptor has been cloned yet. Pharmacological evidence, however, suggests that the putative EET receptors may be linked to adenyl cyclase, cAMP and protein kinase A (PKA) pathway (Wong *et al*, 2000).

Our finding that sEH inhibition is protective against ischemic stroke is consistent with human genetic studies demonstrating that genetic polymorphisms in *EPHX2*, the gene that encodes for sEH, are linked to cardiovascular disease risk, including stroke (Fornage *et al*, 2005), coronary heart disease (Lee *et al*, 2006) and hypertension (Fornage *et al*, 2002). In summary, the current study provides the first description of sEH expression in brain tissue and the first characterization of AUDA-BE as a useful agent in the treatment of stroke brain damage. Our findings suggest that sEH is abundantly expressed in neurons, plays an important role in protection from cerebral ischemic injury and may serve as a potential therapeutic target in post-stroke brain damage.

References

Alkayed NJ, Birks EK, Hudetz AG, Roman RJ, Henderson L, Harder DR (1996*a*) Inhibition of brain P-450 arachidonic acid epoxygenase decreases baseline cerebral blood flow. *Am J Physiol* 271:H1541–6

Alkayed NJ, Birks EK, Narayanan J, Petrie KA, Kohler-Cabot AE, Harder DR (1997) Role of P-450 arachidonic acid epoxygenase in the response of cerebral blood flow to glutamate in rats. *Stroke* 28:1066–72

Alkayed NJ, Goto S, Sugo N, Joh HD, Klaus J, Crain BJ, Bernard O, Traystman RJ, Hurn PD (2001) Estrogen and Bcl-2: gene induction and effect of transgene in experimental stroke. *J Neurosci* 21:7543–50

Alkayed NJ, Goyagi T, Joh HD, Klaus J, Harder DR, Traystman RJ, Hurn PD (2002) Neuroprotection and P4502C11 upregulation after experimental transient ischemic attack. *Stroke* 33:1677–84

Alkayed NJ, Narayanan J, Gebremedhin D, Medhora M, Roman RJ, Harder DR (1996*b*) Molecular characterization of an arachidonic acid epoxygenase in rat brain astrocytes. *Stroke* 27:971–9

Borhan B, Mebrahtu T, Nazarian S, Kurth MJ, Hammock BD (1995) Improved radiolabeled substrates for soluble epoxide hydrolase. *Anal Biochem* 231:188–200

Brand-Schieber E, Falck JF, Schwartzman M (2000) Selective inhibition of arachidonic acid epoxidation *in vivo*. *J Physiol Pharmacol* 51:655–72

Chen JK, Capdevila J, Harris RC (2001) Cytochrome p450 epoxygenase metabolism of arachidonic acid inhibits apoptosis. *Mol Cell Biol* 21:6322–31

Draper AJ, Hammock BD (1999) Soluble epoxide hydrolase in rat inflammatory cells is indistinguishable from soluble epoxide hydrolase in rat liver. *Toxicol Sci* 50:30–5

Enayetallah AE, French RA, Thibodeau MS, Grant DF (2004) Distribution of soluble epoxide hydrolase and of cytochrome P450 2C8, 2C9, and 2J2 in human tissues. *J Histochem Cytochem* 52:447–54

Fleming I, Fisslthaler B, Michaelis UR, Kiss L, Popp R, Busse R (2001) The coronary endothelium-derived hyperpolarizing factor (EDHF) stimulates multiple signalling pathways and proliferation in vascular cells. *Pflugers Arch* 442:511–8

Folch J, Ascolii, Lees, Meath JA, Lebaron N (1951) Preparation of lipide extracts from brain tissue. *J Biol Chem* 191:833–41

Fornage M, Hinojos CA, Nurowska BW, Boerwinkle E, Hammock BD, Morisseau CH, Doris PA (2002) Polymorphism in soluble epoxide hydrolase and blood pressure in spontaneously hypertensive rats. *Hypertension* 40:485–90

Fornage M, Lee CR, Doris PA, Bray MS, Heiss G, Zeldin DC, Boerwinkle E (2005) The soluble epoxide hydrolase gene harbors sequence variation associated with susceptibility to and protection from incident ischemic stroke. *Hum Mol Genet* 14:2829–37

Imig JD, Zhao X, Zaharis CZ, Olearczyk JJ, Pollock DM, Newman JW, Kim IH, Watanabe T, Hammock BD (2005) An orally active epoxide hydrolase inhibitor lowers blood pressure and provides renal protection in salt-sensitive hypertension. *Hypertension* 46:975–81

Junier MP, Dray F, Blair I, Capdevila J, Dishman E, Falck JR, Ojeda SR (1990) Epoxygenase products of arachidonic acid are endogenous constituents of the hypothalamus involved in D2 receptor-mediated, dopamine-induced release of somatostatin. *Endocrinology* 126:1534–40

Kim IH, Morisseau C, Watanabe T, Hammock BD (2004) Design, synthesis, and biological activity of 1,3-disubstituted ureas aspotent inhibitors of the soluble epoxide hydrolase of increased water solubility. *J Med Chem* 47:2110–22

Kim IH, Nishi K, Tsai HJ, Bradford T, Koda Y, Watanabe T, Morisseau C, Blanchfield J, Toth I, Hammock BD (2007) Design of bioavailable derivatives of 12-(3-adamantan-1-yl-ureido)dodecanoic acid, a potent inhibitor of the soluble epoxide hydrolase. *Bioorg Med Chem* 15:312–23

Kozak W, Kluger MJ, Kozak A, Wachulec M, Dokladny K (2000) Role of cytochrome P-450 in endogenous antipyresis. *Am J Physiol Regul Integr Comp Physiol* 279:R455–60

Krotz F, Riexinger T, Buerkle MA, Nithipatikom K, Gloe T, Sohn HY, Campbell WB, Pohl U (2004) Membrane-potential-dependent inhibition of platelet adhesion to endothelial cells by epoxyeicosatrienoic acids. *Arterioscler Thromb Vasc Biol* 24:595–600

Lee CR, North KE, Bray MS, Fornage M, Seubert JM, Newman JW, Hammock BD, Couper DJ, Heiss G, Zeldin DC (2006) Genetic variation in soluble epoxide hydrolase (EPHX2) and risk of coronary heart disease: The Atherosclerosis Risk in Communities (ARIC) study. *Hum Mol Genet* 15:1640–9

Liu M, Alkayed NJ (2005) Hypoxic preconditioning and tolerance via hypoxia inducible factor (HIF) 1 alpha-linked induction of P450 2C11 epoxygenase in astrocytes. *J Cereb Blood Flow Metabol* 25:939–48

Liu M, Hurn PD, Alkayed NJ (2004) Cytochrome P450 in neurological disease. *Curr Drug Metab* 5:225–34

Morisseau C, Goodrow MH, Newman JW, Wheelock CE, Dowdy DL, Hammock BD (2002) Structural refinement of inhibitors of urea-based soluble epoxide hydrolases. *Biochem Pharmacol* 63:1599–608

Newman JW, Morisseau C, Hammock BD (2005) Epoxide hydrolases: their roles and interactions with lipid metabolism. *Prog Lipid Res* 44:1–51

Newman JW, Morisseau C, Harris TR, Hammock BD (2003) The soluble epoxide hydrolase encoded by EPXH2 is a bifunctional enzyme with novel lipid phosphate phosphatase activity. *Proc Natl Acad Sci USA* 100:1558–63

Node K, Huo Y, Ruan X, Yang B, Spiecker M, Ley K, Zeldin DC, Liao JK (1999) Anti-inflammatory properties of cytochrome P450 epoxygenase-derived eicosanoids. *Science* 285:1276–9

Ospina JA, Krause DN, Duckles SP (2002) 17 beta-estradiol increases rat cerebrovascular prostacyclin synthesis by elevating cyclooxygenase-1 and prostacyclin synthase. *Stroke* 33:600–5

Potente M, Fisslthaler B, Busse R, Fleming I (2003) 11,12-Epoxyeicosatrienoic acid-induced inhibition of FOXO factors promotes endothelial proliferation by down-regulating p27Kip1. *J Biol Chem* 278:29619–25

Schmelzer KR, Kubala L, Newman JW, Kim IH, Eiserich JP, Hammock BD (2005) Soluble epoxide hydrolase is a therapeutic target for acute inflammation. *Proc Natl Acad Sci USA* 102:9772–7

Seubert J, Yang B, Bradbury JA, Graves J, Degraff LM, Gabel S, Gooch R, Foley J, Newman J, Mao L, Rockman HA, Hammock BD, Murphy E, Zeldin DC (2004) Enhanced postischemic functional recovery in CYP2J2 transgenic hearts involves mitochondrial ATP-sensitive K+ channels and p42/p44 MAPK pathway. *Circ Res* 95:506–14

Shin JH, Engidawork E, Delabar JM, Lubec G (2005) Identification and characterisation of soluble epoxide hydrolase in mouse brain by a robust protein biochemical method. *Amino Acids* 28:63–9

Spiecker M, Liao JK (2005) Vascular protective effects of cytochrome p450 epoxygenase-derived eicosanoids. *Arch Biochem Biophys* 433:413–20

Watanabe T, Hammock BD (2001) Rapid determination of soluble epoxide hydrolase inhibitors in rat hepatic microsomes by high-performance liquid chromatography with electrospray tandem mass spectrometry. *Anal Biochem* 299:227–34

Watanabe T, Schulz D, Morisseau C, Hammock BD (2006) High-throughput pharmacokinetic method: cassette dosing in mice associated with minuscule serial bleedings and LC/MS/MS analysis. *Anal Chim Acta* 559:37–44

Wong PY, Lai PS, Falck JR (2000) Mechanism and signal transduction of 14 (R), 15 (S)-epoxyeicosatrienoic acid (14,15-EET) binding in guinea pig monocytes. *Prostaglandins Other Lipid Mediat* 62:321–33

Yu Z, Davis BB, Morisseau C, Hammock BD, Olson JL, Kroetz DL, Weiss RH (2004) Vascular localization of soluble epoxide hydrolase in the human kidney. *Am J Physiol Renal Physiol* 286:F720–6

Zeldin DC (2001) Epoxygenase pathways of arachidonic acid metabolism. *J Biol Chem* 276:36059–62

Zhao X, Yamamoto T, Newman JW, Kim IH, Watanabe T, Hammock BD, Stewart J, Pollock JS, Pollock DM, Imig JD (2004) Soluble epoxide hydrolase inhibition protects the kidney from hypertension-induced damage. *J Am Soc Nephrol* 15:1244–53

Zheng J, Plopper CG, Lakritz J, Storms DH, Hammock BD (2001) Leukotoxin-diol: a putative toxic mediator involved in acute respiratory distress syndrome. *Am J Respir Cell Mol Biol* 25:434–8

Supplementary Information accompanies the paper on the Journal of Cerebral Blood Flow & Metabolism website (http://www.nature.com/jcbfm)

SOLUBLE EPOXIDE HYDROLASE: A NOVEL THERAPEUTIC TARGET IN STROKE

Wenri Zhang[*], Ines Koerner[*], Ruediger Noppens[*], Marjorie Grafe[**], Hsing-Ju Tsai[†], Christophe Morisseau[†], Ayala Luria[†], Bruce D. Hammock[†], John R. Falck[‡], Nabil J. Alkayed[*]

[*]Department of Anesthesiology & Peri-Operative Medicine and [**]Department of Pathology, Oregon Health & Science University, Portland, OR

[†]Department of Entomology and UCD Cancer Center, University of California, Davis, CA.

[‡]Department of Biochemistry, UT Southwestern Medical Center, Dallas, TX

SUPPLEMENTAL MATERIALS AND METHODS

Studies with animals were conducted in accordance with the National Institute of Health guidelines for the care and use of animals in research and protocols were approved by Animal Care and Use Committee of Oregon Health and Science University, Portland, Oregon.

Analysis of sEH inhibitors in brain tissue extracts

12-(3-Adamantan-1-yl-ureido)-dodecanoic acid butyl ester (AUDA-BE) was dissolved in sesame oil and administered intraperitoneally (*i.p.*, 10mg/kg) to C57Bl/6 mice (20-26 g). A second set of animals was injected with sesame oil alone (vehicle). Mice were decapitated; and brain tissue samples were collected at 1, 3, 6, and 24 hours after administration with two mice analyzed for each time point. The sEH inhibitor AUDA-BE and its equally active metabolite 12-(3-adamantyl-ureido)-dodecanoic acid (AUDA) or the inactive metabolite, 12-(3-adamantyl-ureido)-butyl acid

(AUBA) were measured in brain tissue homogenates. Briefly, brain tissue samples were flash frozen in liquid nitrogen and were ground with a motor and pestle. Tissue homogenates were spiked with a surrogate internal standard (ADU,1-adamantyl-3-decyl urea, 100ng/ml), and the samples were extracted three times with chloroform, methanol and water (2:1:1) (*Folch et al. J Biol Chem. 1951;191:833-41*). After extraction, samples were dried under N_2, and reconstituted with methanol that contained the internal standard (CUDA, 1-cyclohexyl-3-dodecanoic acid urea, 500 ng/ml). The concentration of sEH inhibitors and metabolites were quantified in extracts using HPLC with positive mode electrospray ionization and tandem mass spectrometry (ESI-MS/MS). Analytes were quantified on a 5-point curve with internal standard methods. Surrogate recoveries were evaluated by quantification against the internal standard as described previously (*Watanabe T et al. Anal Chim Acta. 2006;559:37-44*). Surrogate recoveries in brain tissue homogenates were relatively similar but approximately 30% with only two independent experiments from two individual animals in each time point injected with AUDA-BE (10mg/kg) or vehicle alone (sesame oil) . The analysis of reagent blanks, matrix spikes, and analytical replicates were used to document the stability of the method during this study. Molecular ion and transition ions for the analytes were as followed, AUDA-BE (449.2>272.2), AUDA (393.1>135), AUBA (281.2>104), surrogate compound ADU, 1-adamantyl-3-decyl urea (335.1>135) and internal standard CUDA (341.2>216.2).

Pharmacokinetic Parameter Analysis for sEH inhibitors

The pharmacokinetic parameters were obtained by fitting the blood concentration-time data to a non-compartmental model with the WinNonlin software (Pharsight, Mountain View, CA). Parameters estimated included the time of maximum concentration (T_{max}), the maximum concentration (C_{max}), elimination half-life ($T_{1/2}$), area under the concentration-time curve to

terminal time (AUC_t) and the mean residence time (MRT). See Table S1. A semilog plot of the data in Figure 3 is linear supporting a non-compartmental model.

SUPPLEMENTAL RESULTS

In order to determine sEH inhibitory effect in the brain, the level of sEH inhibitors was first examined in brain extracts (Fig. S1). Brain tissues were homogenized and inhibitors were extracted with methanol and chloroform (*Folch et al. J Biol Chem. 1951;191:833-41*). Although that the recovery of the extracted compounds from the brain was low, it is clearly seen that AUDA accumulated in brain tissue within the first six hours after a single *i.p.* injection of 10mg/kg AUDA-BE (Fig. S1). AUDA was first seen after one hour post injection and reached maximum levels at three hours. Slow degradation of AUDA was observed over the following twenty four hours with a mean residence time (MRT) of six hours. Only 3 pmol/g tissue of AUDA were measured at 24 hours. AUDA-BE was not detected in the brain tissue. AUBA was not measured in these samples since the extraction method is not adequate for hydrophilic compounds (Fig. S1). Pharmacokinetic analysis of AUDA in plasma and brain tissue is summarized in Table S1. As shown, the maximum concentration of AUDA in plasma was measured as 52 nM, while brain maximum concentration was 105 nM (Table S1). The time that AUDA reached maximum concentration was calculated as one hour in plasma samples followed by three hours in brain tissue homogenates, and the mean residence time was nine hours in plasma samples and six hours in brain tissue homogenates (Table S1). AUDA accumulates in brain few hours after injection. These data are consistent with the AUDA-BE ester penetrating membranes quickly, being hydrolyzed to AUDA and AUDA only leaving the brain tissue slowly and being slowly metabolized. Alternatively AUDA could be taken up selectively by the brain. With this particular method, hydrophilic compounds as AUBA cannot be extracted and

measured, while it is most likely that AUDA is degraded by β-oxidation to less active compounds that do not reach biological effective levels in plasma. In plasma samples, the maximum concentration of AUDA is lower than the brain extracts but the half time of elimination and mean residence time both are longer in plasma tissue extracts that likely is a result of the degradation of AUDA-BE to AUDA by esterases.

Table S1. Pharmacokinetic parameters of AUDA in plasma and brain tissue samples.

AUDA	Plasma Samples	Brain tissue Samples
C_{max} (pmol/mL)[a]	52	105
T_{max} (hr) [b]	1.0	3.0
$T_{1/2}$ (hr) [c]	7.2	4.2
AUC (hr*pmol/mL)[d]	582	84
MRT (hr) [e]	9.1	6.0

PK parameters calculated by WinNonlin 5.1 software (Pharsight, Mountain View, CA) with 0-24 hour data points. R^2=0.996 and adjusted R^2=0.995 for $T_{1/2}$ calculations.

[a]Maximum concentration.

[b]Time of maximum concentration.

[c]Elimination half-time.

[d]Area under the concentration (0-24).

[e]Mean residence time.

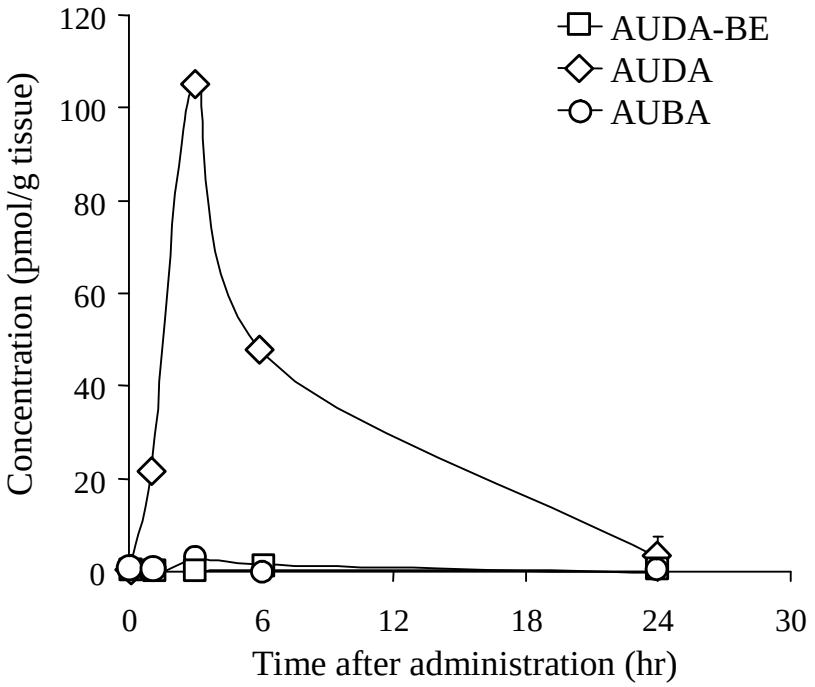

Fig. S1. AUDA concentration in brain tissue extracts. Mice, injected with 10mg/kg AUDA-BE have clearly measurable levels of AUDA but not of AUDA-BE in brain extracts. **AUBA was not detected since the extraction method is not appropriate for hydrophilic compounds**. Results are mean ±SEM of two mice from each treatment and time point.